analytical chemistry

PURDUE UNIVERSITY

Subscriber access provided by Purdue University Libraries

Article

Ultrasmall Organic Nanoparticles with Aggregation Induced Emission and Enhanced Quantum Yield for Fluorescence Cell Imaging

Suying Xu, Xilin Bai, Jingwen Ma, Minmin Xu, Gaofei Hu, Tony D. James, and Leyu Wang

Anal. Chem., **Just Accepted Manuscript** • DOI: 10.1021/acs.analchem.6b02032 • Publication Date (Web): 28 Jun 2016

Downloaded from http://pubs.acs.org on June 28, 2016

Just Accepted

"Just Accepted" manuscripts have been peer-reviewed and accepted for publication. They are posted online prior to technical editing, formatting for publication and author proofing. The American Chemical Society provides "Just Accepted" as a free service to the research community to expedite the dissemination of scientific material as soon as possible after acceptance. "Just Accepted" manuscripts appear in full in PDF format accompanied by an HTML abstract. "Just Accepted" manuscripts have been fully peer reviewed, but should not be considered the official version of record. They are accessible to all readers and citable by the Digital Object Identifier (DOI®). "Just Accepted" is an optional service offered to authors. Therefore, the "Just Accepted" Web site may not include all articles that will be published in the journal. After a manuscript is technically edited and formatted, it will be removed from the "Just Accepted" Web site and published as an ASAP article. Note that technical editing may introduce minor changes to the manuscript text and/or graphics which could affect content, and all legal disclaimers and ethical guidelines that apply to the journal pertain. ACS cannot be held responsible for errors or consequences arising from the use of information contained in these "Just Accepted" manuscripts.

ACS Publications

Analytical Chemistry is published by the American Chemical Society. 1155 Sixteenth Street N.W., Washington, DC 20036

Published by American Chemical Society. Copyright © American Chemical Society. However, no copyright claim is made to original U.S. Government works, or works produced by employees of any Commonwealth realm Crown government in the course of their duties.

Ultrasmall Organic Nanoparticles with Aggregation Induced Emission and Enhanced Quantum Yield for Fluorescence Cell Imaging

Suying Xu†[1], Xilin Bai†[1], Jingwen Ma†, Minmin Xu†, Gaofei Hu†, Tony D. James‡ and Leyu Wang*†

†State Key Laboratory of Chemical Resource Engineering, Beijing Key Laboratory of Environmentally Harmful Chemical Analysis, Beijing University of Chemical Technology, Beijing 100029, P. R. China, Fax:(86)10-64427869

Email: lywang@mail.buct.edu.cn

‡Department of Chemistry, University of Bath, Claverton Down, Bath, BA2 7AY, United Kingdom

ABSTRACT: Using fluorescence probes for biomedical imaging has attracted significant attention over recent years owing to their high resolution at cellular level. The probes are available in many formats including small particle-size based imaging agents which are considered to be promising candidates, due to their excellent stabilities. Yet, concerns over the potential cytotoxicity effects of inorganic luminescent particles have led to questions about their suitability for imaging applications. Exploration of alternatives inspired us to use organic fluorophores with aggregation-induced emission (AIE), prepared by functionalizing the amine group on tetraphenylethene with 3,5-bis(trifluoromethyl)phenyl isocyanate. The as-synthesized novel AIE fluorophore (TPE-F) display enhanced quantum yield and longer lifetime as compared with its counterparts (TPE-AM). Furthermore, the TPE-F was encapsulated into small-size organic nanoparticles (dynamic light scattering size, ~10 nm) with polysuccinimide (PSI). The biocompatibility, excellent stability, bright fluorescence and selective cell-targeting of these NPs enable the as-prepared TPE-F NPs suitable for specific fluorescence cell imaging.

INTRODUCTION

Optical tags including organic[1-3] and inorganic[4-7] labels have been widely investigated for chemical sensing,[8-12] studying crucial biological processes such as protein-protein interaction, metastasis of cancerous cells and real-time monitoring of drug/gene delivery.[13-18] Among the various optical imaging agents, particle-based imaging agents[5-7] are of great interest since organic molecular dyes often suffers from short retention time and are subject to photo-bleaching.[19, 20] However, most particle-based fluorophores are composed of inorganic species, even some toxic heavy metal cations, of which the potential cytotoxicity effects have greatly impaired their application.[21, 22] Encapsulation of organic dye molecules into nanoparticles (NPs) may afford a promising strategy to extend the circulation life-time as particle-based agents and reduce the potential cytotoxicity.[23] However, the fluorescence intensity of conventional fluorophores tends to decrease when they are in in close contact; a common phenomenon known as aggregation-caused quenching (ACQ), which presents a dilemma for conventional fluorophores used in biomedical imaging.[24]

Recently, opposite to the aforementioned ACQ effect, fluorescent molecules with aggregation-induced emission (AIE) feature, that is, the compound is non-emissive in solution but highly fluorescent once in its aggregated state, have been widely investigated for bio-imaging.[25-28] One prototypical compound with AIE properties is tetraphenylethene (TPE), a central olefin stator with four peripheral aromatic rotors connected by single-bonds. Owing to the dynamic rotation of the aromatic rotors as well as twisting motion, the exciton energy is non-radioactively dissipated when in its free form. While in an aggregated state, radiationless relaxation pathways are restricted, thus facilitating the fluorescence emission of TPE.[29] By taking advantage of this property, compounds with AIE properties could accommodate encapsulation in particles while still maintaining fluorescence emission. Indeed, researchers have explored the adaptability for constructing luminescent particles, which show low cytotoxicity and good stability in bioimaging applications.[23, 30-38] Recently, it was also found that the different packing of AIE compounds in the solid state affects the optical properties.[33] We envisaged that fabrication of nanoparticle with small particle size would afford a tight packing of AIE compounds, which may increase the quantum

yields of the afforded organic particles. In another aspect, nanoparticle-based imaging agents with hydrodynamic diameters in the range of 5–10 nm are considered to be optimal since larger particles would accumulate in the liver and spleen *via* non-specific interactions.[39, 40] Herein, we prepared fluorine containing AIE compound (TPE-F) and encapsulated it in small size NPs, which were also labeled with a cell-targeting peptide (Arg-Gly-Asp, RGD). The acquired luminescent NPs display enhanced luminescence intensities and good stability and have been successfully utilized for targeted cellular imaging of HeLa cells.

EXPERIMENTAL SECTION

Chemicals and Reagents. General chemicals were of the highest grade available (at least analytical grade) and used as received without further purification. Absolute ethanol, methanol, chloroform, dimethylformamide (DMF), NaOH, $NaH_2PO_4{\cdot}2H_2O$, and $Na_2HPO_4{\cdot}12H_2O$ were supplied by Beijing Chemical Reagent Company. Polysuccinimide (PSI, Mw~6000) was obtained from Shijiazhuang Desai Chemical Company (China). Oleylamine (OAm) was purchased from Sigma-Aldrich. *4,4′*-Diaminobenzophenone and *3,5*-bis (trifluoromethyl) phenyl isocyanate were supplied by J&K Scientific LTD. Ethyl dimethylaminopropyl carbodiimide solution (EDC), N-Hydroxysuccinimide (NHS), and methyl thiazolyl tetrazolium (MTT) were purchased from Sigma-Aldrich. Deionized (DI) water was used throughout all experiments.

Preparation of TPE-AM. The *4,4′,4″,4‴*-(ethene-*1,1,2,2*-tetrayl)tetraaniline (TPE-AM) was prepared by following previously reported procedures with slight modification.[25] In brief, *4,4′*-diaminobenzophenone (0.4 g, 1.8 mmol) was dissolved in concentrated hydrochloric acid (18 mL) at 60 °C under stirring, followed by the addition of Tin powder (1.2 g, 10 mmol) and the reaction mixture was stirred at 75 °C for 5 h. After cooling, the mixture was vacuum filtrated and washed by NaOH (1 M) and H_2O. After drying overnight at room temperature, TPE-AM was obtained as a yellowish powder (228 mg) in 65% yield. ^{1}H NMR (400 MHz, d_6-DMSO) δ (TMS, ppm): 6.59 (d, J = 8.72 Hz, 8H), 6.27 (d, J = 8.36 Hz, 8H), 4.85 (s, 8H)

Preparation of TPE-F. Compound *1,1′,1″,1‴*-(ethene-*1,1,2,2*-tetrayltetrakis(benzene-*4,1*-diyl))tetrakis(*3*-(*3,5*-bis(trifluoromethyl)phenyl)urea) (TPE-F) was readily synthesized by reacting TPE-AM with *1*-isocyanato-*3,5*-bis(trifluoromethyl)benzene. Specifically, 80 mg (0.2 mmol) of TPE-AM was dissolved in 60 mL of dichloromethane, then 3,5-bis (trifluoromethyl) phenyl isocyanate (160 μL, 0.9 mmol) in 5 mL of dichloromethane was added dropwise and stirred for 30 min in ice-bath. The reaction mixture was then refluxed for 3 h. Thereafter, the organic phase was concentrated under reduced pressure and washed by dichloromethane (DCM). Finally, the product was dried at room temperature to afford a yellowish powder (125 mg) in 44% yield. ^{1}H NMR (400 MHz, d_6-DMSO) δ(TMS, ppm): 9.38 (s, 4H), 8.96 (s, 4H), 8.12 (s, 8H), 7.64 (s, 4H), 7.28 (d, J = 8.48Hz, 8H), 6.93 (d, J = 8.4Hz, 8H); ^{19}F NMR(376 MHz, d_6-DMSO) δ($CFCl_3$, ppm): -61.68 (C_6H_5-CF_3); HR-MS (m/z): M^+, calcd. for $C_{62}H_{37}F_{24}N_8O_4$, 1413.2549; found, 1413.2489

Preparation of hydrophilic TPE-AM@PSI_{OAM} NPs. 1.0 mL of chloroform colloidal solution containing oleylamine functionalized polysuccinimide[41] (PSI_{OAm}, see Supporting Information for synthesis of PSI_{OAm}) (38 mg of PSI_{OAm} and 1.0 mL of methanol solution containing TPE-AM (0.3 mg) was added into 10mL NaOH (5 mM) aqueous solution under ultrasonication (350 W, 6 min). Afterwards, the chloroform and methanol was removed by evaporating at 45 °C for 30 min. Similarly, TPE-F was treated with the above-mentioned method for TPE-F@PSI_{OAm} NPs.

Cell imaging. HeLa cells were seeded on a sterilized glass cover slide and cultured in a 12-well cell culture plate overnight under recommended conditions at 37 °C in 5% CO_2-humiditied incubator. Then, the TPE-F@PSI_{OAm}-RGD stock solution was added into the cell culture well with a final concentration of 30 μg/mL. The HeLa cells were incubated with the TPE-F@PSI_{OAm}-RGD for another 6 h. As a control, TPE-F@PSI_{OAm} without RGD target peptide was incubated with the HeLa cells under the same condition. Thereafter, the cells on the glass slide were washed with phosphate buffer saline (PBS, pH 7.4, 20 mM) and fixed in 4% paraformaldehyde solution for 15 min. The fluorescence imaging based on the fluorescence of TPE-F was conducted on an EVOS FL microscopes system (Life Technologies) with excitation wavelength at 360 nm and emission at 447 nm.

RESULTS AND DISCUSSION

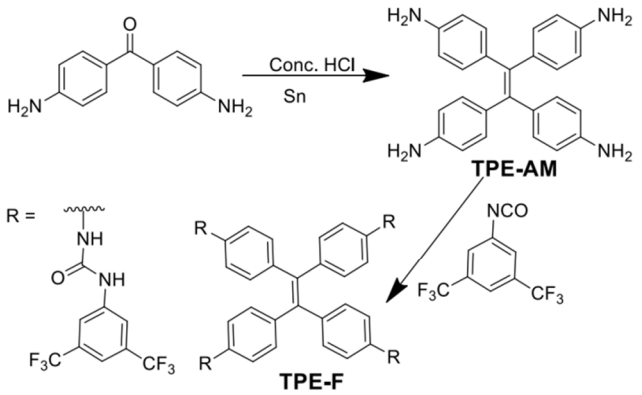

Scheme 1. Reaction procedures for preparation of TPE-F.

Compound TPE-AM was synthesized using the previously reported method.[42] The TPE-F compound was prepared by facile reaction of TPE-AM with *1*-isocyanato-*3,5*-bis(trifluoromethyl)benzene (Scheme 1). The compounds were confirmed using nuclear magnetic resonance (NMR) and mass spectrometry (MS), and given in the Supporting Information Figure S1-S4. Both TPE-AM and TPE-F display weak emission in pure methanol solution, but their optical properties follow the typical behavior of AIE probes when varying water fractions (Figure 1 and 2). More specifically, for TPE-AM, the emission intensity remained unchanged with water fraction less than 80 vol%, but significantly enhanced with further increase of the water fraction. The emission intensity increased up to ~125 fold when compared to that in pure methanol, when the water fraction reaches 90 vol%. As for TPE-F, the emission intensity increased about 143 fold when compared to that for pure methanol. The conjugation of TPE-AM with 3,5-bis(trifluoromethyl) phenyl isocyanate further extends the conjugation system and also increases the rigidity of

the molecule, thus producing significantly enhanced emission intensities.

Interestingly, the TPE-F compound displays its maximal emission intensities with the water fraction at 40% (Figure 2). If the water fraction was further increased, the emission intensity was reduced, which can probably be ascribed to the precipitation of the TPE-F aggregates due to poor solubility of the TPE-F compound, as shown by the photographic images under UV light (Figure S5). These issue could be solved by encapsulating the TPE-F into a hydrophobic particle core using hydrophilic and biocompatible PSI_{OAM}, which in one aspect, increases the packing density, meanwhile avoiding any undesired precipitation.

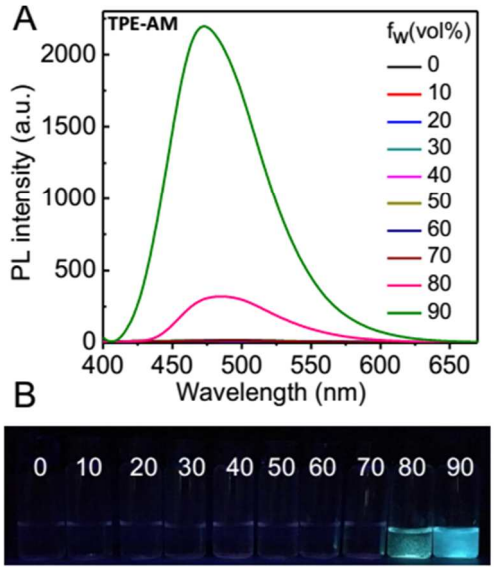

Figure 1. (A) Fluorescent spectra of compound TPE-AM at different water fraction (f_w); (B) Photographs of TPE-AM solution with different water fraction under UV light. [TPE-AM] = 50 μg/mL; λ_{ex} = 365 nm.

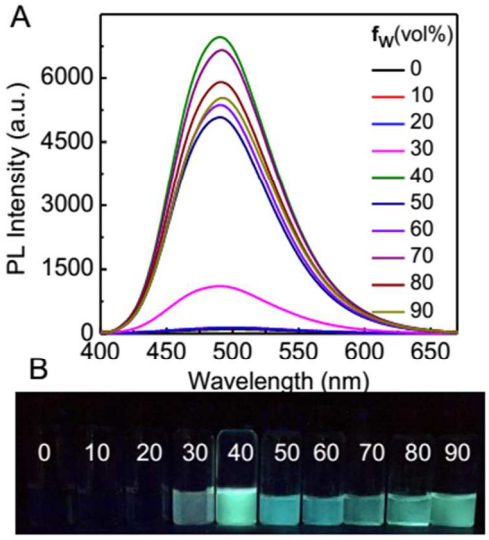

Figure 2. A) Fluorescent spectra of compound TPE-F at different water fraction; (B) Photographs of TPE-F solution with different water fractions under UV light. [TPE-F] = 50 μg/mL; λ_{ex} = 365 nm.

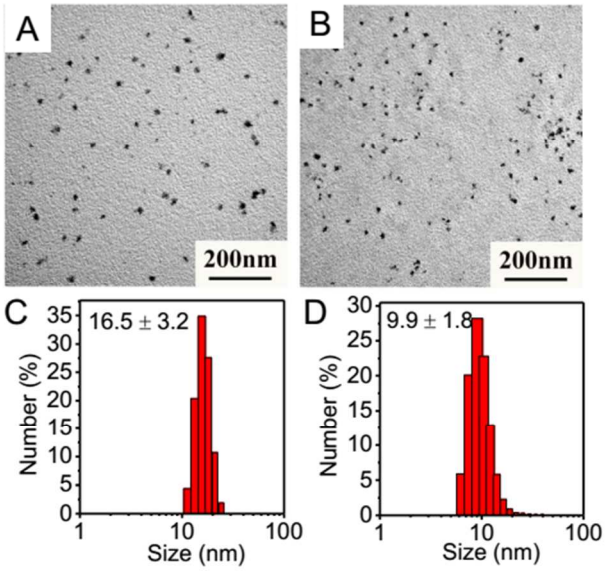

Figure 3. TEM images (A, B) and DLS (C, D) analysis of TPE-AM@PSI_{OAm} (A, C) and TPE-F@PSI_{OAm} (B, D), respectively.

To this end, fabrication of luminescent AIE nanoaggregates was achieved by using oleylamine functionalized amphiphilic polysuccinimide (PSI_{OAm}). The hydrophobic AIE compounds were encapsulated in the hydrophobic cores of the particles after being subjected to ultrasonication under alkali conditions. The transmission electron microscopy (TEM) images and dynamic light scattering (DLS) results (Figure 3) indicated that the afforded TPE-AM@PSI_{OAm} and TPE-F@PSI_{OAm} have average sizes of 16.5±3.2 and 9.9±1.8 nm, respectively, which are smaller than most of the reported AIE organic particles.[32-35] With respect to the optical properties, the TPE-F@PSI_{OAm} displayed stronger emission intensities when compared with TPE-AM@PSI_{OAm} (Figure 4) at the same concentration, similar to the phenomenon observed in solution. Additionally, increased amounts of AIE compounds would result in much more enhanced emission intensities. The fluorescence quantum yields for TPE-AM@PSI_{OAm} and TPE-F@PSI_{OAm} were measured to be 0.05 and 0.52, respectively when using quinine sulfate as a reference. The observed high quantum yield of TPE-F@PSI_{OAm} originates from the dense packing of the TPE-F in the hydrophobic cores as well as the increased rigidity of the molecule itself. Moreover, the emission intensities of TPE-F@PSI_{OAm} NPs were inert to changes of pH, while the emission of TPE-AM@PSI_{OAm} has a strong pH dependency (Figure S6). This is reasonable given that the amine group is prone to protonation under acidic condition, thus leading to a decrease of electron density for the compounds, this may in turn affect the emission intensity of TPE-AM. In another aspect, fabrication of TPE-F@PSI_{OAm} NPs also offers an effective way to avoid unwanted precipitation observed with isolated TPE-F aggregates in mixed solvents, since the carboxylic acid groups on the amphiphilic PSI_{OAM} allow for good dispersion of the as-prepared TPE-F@PSI_{OAm} NPs (Figure S5).

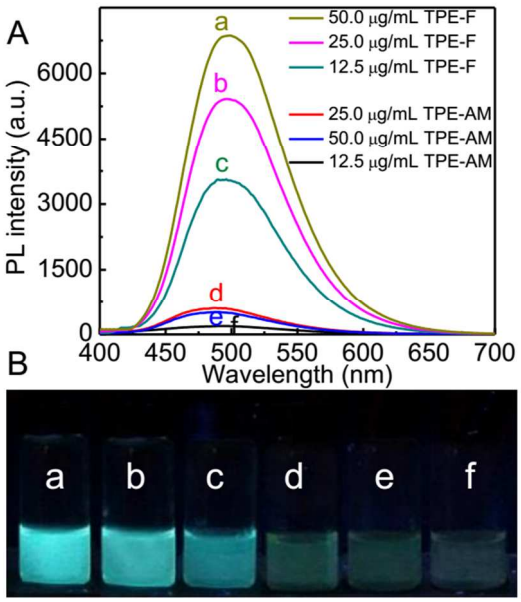

Figure 4. (A) Fluorescent spectra of TPE-F@PSI_{OAm} (a,b,c) and TPE-AM@PSI_{OAm} (d,e,f) at different concentrations: 12.5 (c, f), 25.0 (b,d) and 50.0 μg/mL(a,e), respectively; (B) Photographs of TPE-AM@PSI_{OAm} and TPE-F@PSI_{OAm} solutions at different concentrations: 12.5 (c, f), 25.0 (b, d) and 50.0 μg/mL (a, e), respectively

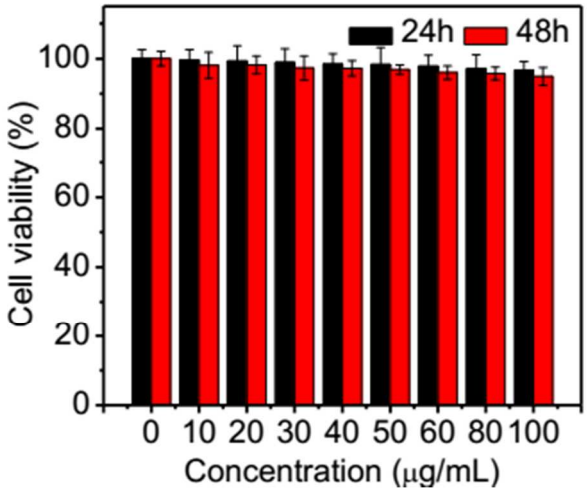

Figure 5. Cell viabilities after treatment with various concentrations of TPE-F@PSI_{OAm}-RGD NPs suspension for 24 and 48 h, respectively.

Furthermore, the RGD moiety was attached to phosphatidyl ethanolamine, which was further employed as co-ligands to prepare TPE-F@PSI_{OAM}-RGD NPs. The cytotoxicity of the TPE-F@PSI_{OAM}-RGD NPs was evaluated *via* the methyl thiazolyltetrazolium (MTT) assay, where HeLa cells were incubated with different amounts of TPE-F@PSI_{OAM}-RGD NPs for 24 and 48 h, respectively (Figure 5). As a control, TPE-F@PSI_{OAM} NPs were treated under identical experimental conditions (Figure S7). As shown in Figure 5 and Figure S7, over 95% cell viability was observed for both types of NPs, showing an ultrahigh biocompatibility. In addition, the emission intensity of TPE-F@PSI_{OAM}-RGD NPs remains constant when left in both phosphate buffer saline (PBS) and DMEM culture media for over one week (Figure S8), indicating their excellent stability. To further demonstrate their performance in bioimaging, HeLa cells were incubated with TPE-F@PSI_{OAm} and TPE-F@PSI_{OAM}-RGD NPs, respectively. As indicated by Figure 6, HeLa cells incubated with TPE-F@PSI_{OAm}-RGD display bright typical AIE emission while those incubated with TPE-F@PSI_{OAM}, no emission was observed, implying the specific targeting ability of the TPE-F@PSI_{OAM}-RGD NPs.

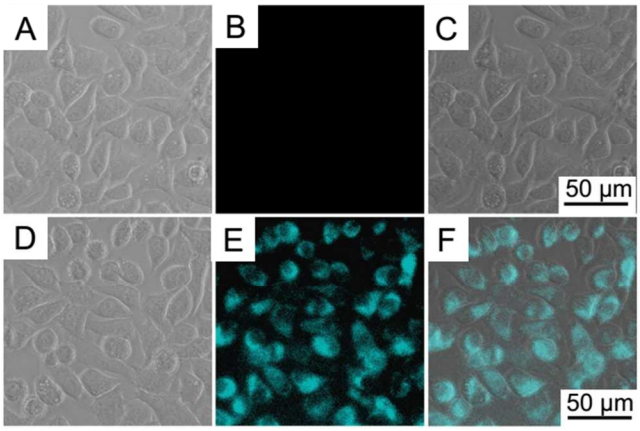

Figure 6. Fluorescence images of HeLa cells cultured with TPE-F@PSI_{OAm} (A,B,C) and TPE-F@PSI_{OAm}-RGD (D, E, F) nanoparticle suspension for 6 hours, respectively.

CONCLUSION

In summary, ultrasmall fluorescent organic NPs with aggregated induced emission and high quantum yields were developed by encapsulating compound AIE-F as the hydrophobic core with an amphiphilic polymer (PSI_{OAm}). The as-prepared NPs display good biocompatibility when compared to conventional inorganic quantum dots, and display excellent stability even in biological medium. Additionally, modification with cell targeting RGD peptide allowed for specific cancer cell imaging, clearly demonstrating the bio-imaging potential of these particles. Currently we are also exploring the potential of using TPE-F for multimodal imaging coupled with ^{19}F magnetic resonance imaging (MRI) by using the fluorine atom on the compound of TPE-F.

ASSOCIATED CONTENT

Supporting Information

Instrumentation, synthesis of PSI_{OAM}, RGD grafting, cell viability tests, NMR and MS results of compound TPE-AM and TPE-F (Figure S1-S4), photographs of TPE-AM and TPE-F solution under UV light (Figure S5), pH influence on the fluorescence (Figure S6), cell viability treated with different concentration of TPE-F@PSI_{OAm} (Figure S7), DLS results and fluorescent intensities changes of TPE-F@PSI_{OAm}-RGD (Figure S8).

AUTHOR INFORMATION

Corresponding Author

lywang@mail.buct.edu.cn (Leyu Wang)

Notes

[1] these two authors contributed equally to this work.

The authors declare no competing financial interest.

ACKNOWLEDGMENT

This research was supported in part by the National Natural Science Foundation of China (Grant Nos. 21475007, 21275015 and 21505003), and the Fundamental Research Funds for the Central Universities (YS1406, buctrc201507 and buctrc201608). We also thank the support from the "Innovation and Promotion Project of Beijing University of Chemical Technology", the "Public Hatching Platform for Recruited Talents of Beijing University of Chemical Technology, the High-Level Faculty Program of Beijing University of Chemical Technology (buctrc201325), and BUCT Fund for Disciplines Construction and Development (Project No. XK1526)".

REFERENCES

(1) Wang, S. G.; Xu, S. Y.; Hu, G. F.; Bai, X. L.; James, T. D.; Wang, L. Y., *Anal. Chem.* **2016,** *88*, 1434-1439.
(2) Huang, S.; He, Q.; Xu, S. Y.; Wang, L. Y., *Anal. Chem.* **2015,** *87*, 5451-5456.
(3) Guo, Z. Q.; Shao, A. D.; Zhu, W. H., *J. Mater. Chem. C* **2016,** *4*, 2640-2646.
(4) Liu, J. L.; Lu, L. L.; Li, A. Q.; Tang, J.; Wang, S. G.; Xu, S. Y.; Wang, L. Y., *Biosens. Bioelectron.* **2015,** *68*, 204-209.
(5) Deng, M. L.; Wang, L. Y., *Nano Res.* **2014,** *7*, 782-793.
(6) Ma, Y. X.; Huang, S.; Deng, M. L.; Wang, L. Y., *ACS Appl. Mater. Inter.* **2014,** *6*, 7790-7796.
(7) Bai, M.; Huang, S. N.; Xu, S. Y.; Hu, G. F.; Wang, L. Y., *Anal. Chem.* **2015,** *87*, 2383-2388.
(8) Wan, Q. Q.; Song, Y. C.; Li, Z.; Gao, X. H.; Ma, H. M., *Chem. Commun.* **2013,** *49*, 502-504.
(9) Ma, Y. X.; Li, H.; Peng, S.; Wang, L. Y., *Anal. Chem.* **2012,** *84*, 8415-8421.
(10) Zhao, Y. Y.; Ma, Y. X.; Li, H.; Wang, L. Y., *Anal. Chem.* **2012,** *84*, 386-395.
(11) Chen, X. X.; Wu, X.; Zhang, P.; Zhang, M.; Song, B. N.; Huang, Y. J.; Li, Z.; Jiang, Y. B., *Chem. Commun.* **2015,** *51*, 13630-13633.
(12) Wu, X.; Li, Z.; Chen, X. X.; Fossey, J. S.; James, T. D.; Jiang, Y. B., *Chem. Soc. Rev.* **2013,** *42*, 8032-8048.
(13) Chen, G. C.; Tian, F.; Zhang, Y.; Zhang, Y. J.; Li, C. Y.; Wang, Q. B., *Adv. Funct. Mater.* **2014,** *24*, 2481-2488.
(14) Hu, F.; Huang, Y. Y.; Zhang, G. X.; Zhao, R.; Yang, H.; Zhang, D. Q., *Anal. Chem.* **2014,** *86*, 7987-7995.
(15) Bai, X.; Wang, S.; Xu, S.; Wang, L., *TrAC-Trend Anal. Chem.* **2015,** *73*, 54-63.
(16) Zhuang, Y.; Huang, F. J.; Xu, Q.; Zhang, M. S.; Lou, X. D.; Xia, F., *Anal. Chem.* **2016,** *88*, 3289-3294.
(17) Bai, M.; Bai, X. L.; Wang, L. Y., *Anal. Chem.* **2014,** *86*, 11196-11202.
(18) Sun, X. L.; Zhai, W. L.; Fossey, J. S.; James, T. D., *Chem. Commun.* **2016,** *52*, 3456-3469.
(19) Medintz, I. L.; Uyeda, H. T.; Goldman, E. R.; Mattoussi, H., *Nat. Mater.* **2005,** *4*, 435-446.
(20) Xu, S. Y.; Huang, S.; He, Q.; Wang, L. Y., *Trac-Trends Anal. Chem.* **2015,** *66*, 72-79.
(21) Hines, M. A.; Scholes, G. D., *Adv. Mater.* **2003,** *15*, 1844-1849.
(22) Resch-Genger, U.; Grabolle, M.; Cavaliere-Jaricot, S.; Nitschke, R.; Nann, T., *Nat. Method* **2008,** *5*, 763-775.
(23) Chen, B.; Feng, G. X.; He, B. R.; Goh, C.; Xu, S. D.; Ramos-Ortiz, G.; Aparicio-Ixta, L.; Zhou, J.; Ng, L. G.; Zhao, Z. J.; Liu, B.; Tang, B. Z., *Small* **2016,** *12*, 782-792.
(24) Lakowicz, J. R., *Principles of Fluorescence Spectroscopy*. Springer US: 2006; p 703.
(25) Mei, J.; Leung, N. L. C.; Kwok, R. T. K.; Lam, J. W. Y.; Tang, B. Z., *Chem. Rev.* **2015,** *115*, 11718-11940.
(26) Hong, Y. N.; Lam, J. W. Y.; Tang, B. Z., *Chem. Soc. Rev.* **2011,** *40*, 5361-5388.
(27) Yuan, W. Z.; Lu, P.; Chen, S. M.; Lam, J. W. Y.; Wang, Z. M.; Liu, Y.; Kwok, H. S.; Ma, Y. G.; Tang, B. Z., *Adv. Mater.* **2010,** *22*, 2159-2163.
(28) Han, A. T.; Wang, H. M.; Kwok, R. T. K.; Ji, S. L.; Li, J.; Kong, D. L.; Tang, B. Z.; Liu, B.; Yang, Z. M.; Ding, D., *Anal. Chem.* **2016,** *88*, 3872-3878.
(29) Zhang, S.; Qin, A. J.; Sun, J. Z.; Tang, B. Z., *Prog. Chem.* **2011,** *23*, 623-636.
(30) Zhu, Z. F.; Qian, J.; Zhao, X. Y.; Qin, W.; Hu, R. R.; Zhang, H. Q.; Li, D. Y.; Xu, Z. P.; Tang, B. Z.; He, S. L., *ACS Nano* **2016,** *10*, 588-597.
(31) Zhao, Q. L.; Li, K.; Chen, S. J.; Qin, A. J.; Ding, D.; Zhang, S.; Liu, Y.; Liu, B.; Sun, J. Z.; Tang, B., *J. Mater. Chem.* **2012,** *22*, 15128-15135.
(32) Li, K.; Qin, W.; Ding, D.; Tomczak, N.; Geng, J. L.; Liu, R. R.; Liu, J. Z.; Zhang, X. H.; Liu, H. W.; Liu, B.; Tang, B. Z., *Sci Rep* **2013,** *3*, 10.
(33) Geng, J. L.; Li, K.; Qin, W.; Ma, L.; Gurzadyan, G. G.; Tang, B. Z.; Liu, B., *Small* **2013,** *9*, 2012-2019.
(34) Wang, Z. L.; Xu, B.; Zhang, L.; Zhang, J. B.; Ma, T. H.; Zhang, J. B.; Fu, X. Q.; Tian, W. J., *Nanoscale* **2013,** *5*, 2065-2072.
(35) Yan, L. L.; Zhang, Y.; Xu, B.; Tian, W. J., *Nanoscale* **2016,** *8*, 2471-2487.
(36) Zhang, X. Q.; Zhang, X. Y.; Wang, S. Q.; Liu, M. Y.; Tao, L.; Wei, Y., *Nanoscale* **2013,** *5*, 147-150.
(37) Zhang, X. Y.; Zhang, X. Q.; Yang, B.; Liu, M. Y.; Liu, W. Y.; Chen, Y. W.; Wei, Y., *Polym. Chem.* **2014,** *5*, 356-360.
(38) Zhang, X. Y.; Wang, K.; Liu, M. Y.; Zhang, X. Q.; Tao, L.; Chen, Y. W.; Wei, Y., *Nanoscale* **2015,** *7*, 11486-11508.
(39) Zhang, Y.; Zhang, Y. J.; Hong, G. S.; He, W.; Zhou, K.; Yang, K.; Li, F.; Chen, G. C.; Liu, Z.; Dai, H. J.; Wang, Q. B., *Biomaterials* **2013,** *34*, 3639-3646.
(40) Blanco, E.; Shen, H.; Ferrari, M., *Nat. Biotechnol.* **2015,** *33*, 941-951.
(41) Huang, S.; Bai, M.; Wang, L. Y., *Sci Rep* **2013,** *3*, 2023-2027.
(42) Gorvin, J. H., *J. Chem. Soc.* **1959**, 678-682.

For Table of Content only